Lateral Control of Hybrid Drones: Near-Optimal Power Disturbance **Aware Policy**

Miroslav Kosanić and Marija Ilić

Abstract—In unmanned aerial vehicle (UAV) systems, achieving extended flight autonomy remains a significant challenge, even in hybrid systems utilizing both fuel and battery as energy sources. To extend the flight time, our paper introduces a novel application of online composite control that achieves fuel savings through disturbance awareness. Our contributions include the derivation of a nonlinear model of the energyconversion dynamics and its connection with lateral dynamics. We discuss how these nonlinearities are linearized through timescale separation based on the operational rates of drone energy sources. The effectiveness of our composite control method is validated through real-world drone flight data. Numerical results show a reduction in fuel usage of approximately 4.5% through a disturbance-aware policy. This paper not only advances the fundamental understanding of composite control for bilinear time-scale separated systems but also opens new directions for research in trajectory optimization for hybrid powertrain systems.

I. INTRODUCTION

Hybrid Powertrain Unmanned Aerial Vehicles (HPUAVs) have matured across various industries, thanks to their enhanced capabilities and extended operational range. Multirotors, as the most prominent HPUAVs, are distinguished by their simplicity, agility, and ability to execute prolonged missions. Their diverse applications range from agricultural operations to sophisticated logistics and infrastructure inspection tasks. A critical aspect of leveraging HPUAVs to their fullest potential is developing holistic dynamic models encompassing the mechanical, electrical, and chemical subsystems. Capturing the system behavior of multi-physics models is important for designing better control algorithms that ensure optimal performance, safety, and extended autonomy. The trade-off is that such modeling adds nonlinearities to the model, which presents a challenge for linear control.

As discussed in [1] there exist many different drone modeling approaches, all of which result in a nonlinear dynamical system characterized by four inputs and six degrees of freedom (three Cartesian coordinates and three orientation angles). Also, these models usually don't consider energy conversion dynamics.

Several works have addressed hierarchical decoupling in drone control dynamics [2, 3]. In [4] based on the dynamics decoupling, the model is linearized, and translational control is bounded in the neighborhood of small Euler angles. In

This work was supported by the MIT Advanced Concepts Committee (ACC) Lincoln Lab Project entitled "Exergy Control for Supplying Missioncritical Loads'

M. Kosanić is with the Department of Electrical Engineering and and Computer Science, MIT, MA 02139, USA kosanic@mit.edu

M. Ilić is with the Department of Electrical Engineering and Computer Science, MIT, MA 02139, USA ilic@mit.edu

work by [5] and [6] the focus was on the linearization of translational dynamics to enhance trajectory-tracking capabilities. The work of [7] introduces auxiliary controls that are dependent on Euler angles, offering a subtle approach to linearization. In the paper, [8] a choice of an alternative rotation matrix is used for linearization purposes.

While linearization is needed for linear control, another important aspect that affects drone performance is understanding the dynamics of energy sources. Omitting the battery performance analysis may result in inaccurate estimates of the real flight time of the drone [9]. The work in [10] integrates a battery-aware model for an accurate analysis of drone energy consumption, where the captured relationship is experimentally derived look-up table. The work presented in [11] introduced an energetic model for quadrotor UAVs, which includes the vehicle dynamics, actuator dynamics, and battery dynamics, integrated with an efficiency function. The nonlinear optimization objective minimized the energy consumption of a quadrotor, subject to boundary conditions and feasibility constraints on the system states and control inputs. Similarly, [12] formulates a combined approach for flight mission planning and recharging, wherein energy expenditure is subject to environmental meteorological conditions.

Even though cited papers acknowledge and show the importance of accounting for energy expenditure and the effects of inaccurate models on trajectory tracking, two problems arise. First, the models of energy conversion are not dynamic, and this relationship changes due to environmental effects. Second, most of the literature focuses on electricpowered drones, where the problem of trajectory tracking dynamics is modeled as nonlinear and then linearized based on hierarchical decoupling, relying on the assumed stability of mechanical dynamics controllers.

Through the concept of power conservation across the drone mechanical and powertrain subsystems, we introduce a novel model that captures energy conversion dynamics with drone lateral dynamics. By separating drone control into fast (battery dynamics) and slow (fuel reservoir dynamics) components, the model becomes linear. Separation is based on the timescale of the rate at which fuel and battery energy sources operate compared to drone mechanics.

The implications of our paper are three-fold. First, we showcase through power conservation how to connect mechanical dynamics with energy conversion dynamics. Second, how the rate at which different energy sources operate affects time-scale separation, and lastly we apply disturbance-aware tracking control and show a decrease in fuel usage that results in fuel savings.

II. NEAR-OPTIMAL CONTROL

Time-critical systems have to adhere to timing constraints, which if not satisfied can lead to system damage and operation failure. In the pursuit of efficiency, especially in timecritical systems affected by disturbances, the theme of nearoptimal composite control remains one of the central topics in control theory [13]-[14]. Drones as such systems have to manage and guarantee strict time requirements to ensure system stability, safety, and reliability. This section outlines the methodology for decomposing singularly perturbed linear systems and discusses modifications to the online policy computed using the Linear-Quadratic Regulator (LQR) in the presence of disturbances.

A. Composite control

We consider a singularly perturbed linear time-invariant system

$$\dot{x}_1 = A_{11}x_1 + A_{12}x_2 + B_1u \tag{1}$$

$$\epsilon \dot{x}_2 = A_{21}x_1 + A_{22}x_2 + B_2u \tag{2}$$

$$y = C_1 x_1 + C_2 x_2 (3)$$

where ϵ is a small positive scalar, the state x is formed by the R^{n_1} and R^{n_2} vectors x_1, x_2 , the control u is an R^m vector and the output y a \mathbb{R}^k vector.

The system of Eqs. (1)-(3) is characterized by a two-timescale property, manifesting n_1 eigenvalues of small magnitude $\mathcal{O}(1)$ and n_2 eigenvalues of large magnitude $\mathcal{O}(1/\epsilon)$. Before achieving a bifurcation of slow and fast dynamics, system Eq. (1) undergoes an approximate decomposition into a slow subsystem comprising n_1 small eigenvalues and a fast subsystem encompassing n_2 large eigenvalues. Within an asymptotically stable regime, the system's transient behavior is predominantly governed by the fast modes associated with the large eigenvalues. After the transient phase, these modes become negligible, and the system's dynamics are predominantly attributed to the slow modes. An assumption of infinitely fast modes, i.e., $\epsilon \to 0$ in Eq. (2), essentially cancels their influence, thereby simplifying Eqs. (1)-(3) to

$$\dot{x}_1 = A_{11}x_1 + A_{12}\bar{x}_2 + B_1u, \qquad x_1(0) = \bar{x}_{10}$$
 (4)

$$0 = A_{21}x_1 + A_{22}\bar{x}_2 + B_2u \tag{5}$$

$$\bar{y} = C_1 x_1 + C_2 \bar{x}_2 \tag{6}$$

Overbar denotes the slow part of all respective variables when $\epsilon = 0$. Under assumption of A_{22} to be invertible, \bar{x}_2 is expressed as

$$\bar{x}_2 = -A_{22}^{-1}(A_{21}\bar{x}_1 + B_2\bar{u}) \tag{7}$$

Substituting into (2), the slow subsystem of (1) is thus defined as:

$$\dot{x}_s = A_0 x_s + B_0 u_s, \qquad x_s(0) = x_{1,0} \tag{8}$$

$$y_s = C_0 x_s + D_0 u_s \tag{9}$$

where $x_s = \bar{x}_1$, $y_s = \bar{y}_1$, $u_s = \bar{u}$ and

$$A_0 = A_{11} - A_{12}A_{22}^{-1}A_{21}, \quad B_0 = B_1 - A_{12}A_{22}^{-1}B_2,$$

 $C_0 = C_1 - C_2A_{22}^{-1}A_{21}, \quad D_0 = -C_2A_{22}^{-1}B_2.$

To obtain the fast subsystem, we assume that the slow variables remain invariant during transients of the fast subsystem, implying $\dot{\bar{x}}_2 = 0$ and $x_1 = \bar{x}$, are constant. Integrating these conditions into Eqs. 2 and 3, we obtain

$$\epsilon \dot{x}_f = A_{22}x_f + B_2u_f, \quad x_f(0) = x_{2,0} - \bar{x}_2(0)$$
 (10)

$$y_f = C_2 x_f \tag{11}$$

where $x_f = x_2 - \bar{x}_2$, $u_f = u - \bar{u}$, and $y_f = y - \bar{y}$ and thus, defining the fast subsystem.

B. Online Policy in Presence of Disturbance

Suppose, like in [15] that each of the previously defined linearly invariant slow and fast subsystems Eqs. (8)-(11) can be discretized and in the following LTI form

$$x_{t+1} = Ax_t + Bu_t + d_t, \quad t = 0, 1, \dots, T - 1$$
 (12)

where $A \in \mathbb{R}^{n \times n}$ is the system state and $B \in \mathbb{R}^{n \times m}$ is the system input matrix, $x_t \in \mathbb{R}^n$ is the system state and $u_t \in \mathbb{R}^m$ is the control input, while $d_t \in \mathbb{R}^n$ is an external disturbance, and T is the time horizon over which the system is controlled. We focus on the disturbances d_t , which if sparse $d_t \neq 0$ if and only if $t \in D$, for some index set $D = \{t_1, t_2, \dots, t_{|D|}\}$, and |D| is cardinality of the set D. The nonzero disturbances are given by $d_k = w_k$, $k \in \{1, \dots, |D|\}$, and are bounded in ℓ_2 norm by $||w_k|| \leq W$

The objective of the online policy is to minimize the cost

$$\mathbb{E}_{d_0,\dots,d_{T-1}} \left(x_T^T Q_T x_T + \sum_{t=0}^{T-1} x_t^T Q x_t + u_t^T R u_t \right)$$
 (13)

where $Q_T, Q \succeq 0$ and $R \succ 0$ with $Q_T, Q \in \mathbb{R}^{n \times n}$ and $R \in \mathbb{R}^{m \times m}$.

With disturbances as $d = 0, \forall t \in [t_0, T]$, the conventional LQR control policy assumes a disturbance-free environment, a simplification that may not be aligned with reality. We assume that disturbances d are independent with zero mean. The optimal disturbance-free policy is an LQR controller [16] of the form $u_t = -K_t x_t$, for t = [0...T), where

$$K_t = (B^{\top} P_{t+1} B + R)^{-1} B^{\top} P_{t+1} A \tag{14}$$

and the P_t comes as the solution of the discrete-time Riccati equation

$$P_{t} = A^{\top} \left(P_{t+1} - P_{t+1} B (B^{\top} P_{t+1} B + R)^{-1} B^{\top} P_{t+1} \right) A + Q$$
(15)

with
$$P_T = Q_T$$
.

In the situation when policy knows the disturbance d_t , the structure of optimal control is modified according to [17]. Under the assumption that the control has complete knowledge (or reliably can predict) of all disturbances d(t), $\forall t \in$ $[t_0, T]$, the optimal policy and cost will be

$$u_t^* = -K_t x_t - (B^\top P_{t+1} B + R)^{-1}$$

$$\times B^\top (P_{t+1} d_{t+1} + \frac{1}{2} v_{t+1})$$
(16)

$$V_t(x) = x^{\top} P_t x + v_t^{\top} x + q_t \tag{17}$$

$$v_t = 2A^{\top} S_t d_t + A^{\top} S_t P_{t+1}^{-1} v_{t+1}$$
(18)

$$q_t = q_{t+1} + d_t^{\top} S_{t+1} d_t + v_{t+1}^{\top} P_{t+1}^{-1} S_t d_t$$

$$-\frac{1}{4}v_{t+1}^{\top}B(B^{\top}P_{t+1}B+R)^{-1}B^{\top}v_{t+1}$$
(19)
$$S_{t} = P_{t+1} - P_{t+1}B(B^{\top}P_{t+1}B+R)^{-1}B^{\top}P_{t+1}$$
(20)

$$S_t = P_{t+1} - P_{t+1}B(B^{\top}P_{t+1}B + R)^{-1}B^{\top}P_{t+1} \quad (20)$$

where $V_t(x)$ is the cost-to-go of a state x at time t, and recurrences $v_t \in \mathbb{R}^n$, $q_t \in \mathbb{R}$ depend only on the noise d_t .

Problem: Extend the flight autonomy of the drone with the hybrid powertrain by incorporating disturbance knowledge in the composite near-optimal control. First, derive the model of the hybrid drone and implement a power disturbance-aware policy for lateral control. Show the impact of disturbance knowledge on fuel savings, measured through the percentage of fuel remaining at the end of the flight compared to the beginning.

The integration of a battery-aware control is expected to yield quantifiable benefits in fuel savings when contrasted with a battery-blind control [18].

III. MODEL DERIVATION AND CONTROL

Our model derivation begins with a detailed examination of the forces exerted on a drone's frame, which is fundamental to understanding its behavior. The drone mechanical model incorporates both translational and rotational movements to provide an in-depth understanding of the drone's dynamics in flight. Next, we obtain fuel reservoir-engine dynamics, which we will call fuel flow dynamics, through the concept of conservation of power, using analogies of multiphysics domain variables, called effort and flow variables [19], of each subsystem interface(port) variables. By adding relevant mechanical equations from the full model, we obtain the state-space model that captures lateral and fuel dynamics. Finally, we decompose the model into fast and slow subsystems, for which composite control can be formulated.

A. Drone Dynamics

We analyze the multi-copter configuration of the hexacopter. It is assumed in this configuration, that the six rotors mixing pattern for the thrust command, is such that odd-numbered rotors have a pitch opposite to the evennumbered rotors. The angular speed of each rotor is denoted by ω_i , $\forall i \in \{1, \dots, 6\}$. The thrust force T_i , for each of the rotors is given by the equation

$$T_i = k_T \omega_i^2 \tag{21}$$

where k_T and k_M are constants empirically determined for a propeller operating under time-stationary environment conditions. The resulting thrust, the sum of each rotor thrust is then

$$T_{thrust} = \sum_{i}^{6} T_i \tag{22}$$

For our hybrid hexacopter, the motor dynamics are significantly faster than the time scales of rigid body dynamics and aerodynamics. This simplifies the model by assuming that T_i can be adjusted instantaneously, neglecting the detailed dynamics of the motors' response time. From the datasheets of the ESC, the relationship between the commanded throttle and each motor thrust output is represented through the polynomial

$$p(x) = -4600x^3 + 10107x^2 - 1198x + 472 (23)$$

where polynomial argument x is the commanded throttle that determines the thrust force of a motor. The resulting forces acting on the drone frame along each of its axis, are as follows

$$F_{\rm x} = T_{\rm thrust}(\cos(\theta)\cos(\psi) + \sin(\phi)\sin(\theta)\sin(\psi)) \tag{24}$$

$$F_{y} = T_{\text{thrust}}(\cos(\theta)\sin(\psi) - \sin(\phi)\sin(\theta)\cos(\psi))$$
 (25)

$$F_{z} = T_{\text{thrust}}(\cos(\phi)\sin(\theta)) \tag{26}$$

where θ is the pitch, ϕ is the roll, and ψ the yaw angle, are used to calculate how this total thrust vector is oriented concerning the drone's body frame. These equations assume that the total thrust vector is initially aligned with the drone's vertical axis and that pitch, roll, and yaw movements tilt this vector accordingly. This representation simplifies the model by not considering the individual thrusts and orientations of each rotor, but instead, it focuses on how the overall orientation of the drone (as determined by yaw, roll, and pitch) affects the direction of the total thrust force.

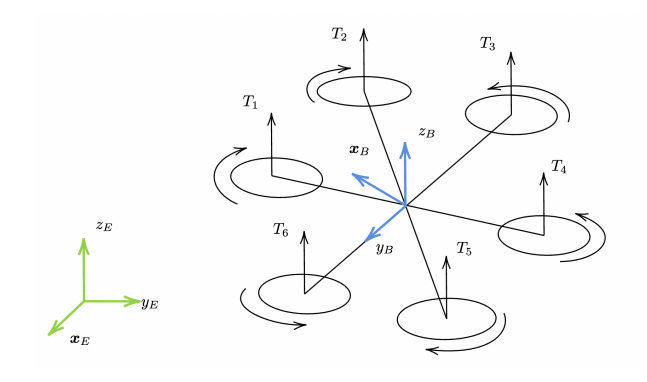


Fig. 1. Reference frames and hexacopter representation

Disturbances acting on a drone's frame are commonly modeled using drag force. The general form of drag force is expressed as

$$F_{\text{drag},i} = \frac{1}{2} \rho v_i^2 C_{D,i} A_i$$
 (27)

where $i \in \{x, y, z\}$ represents directions in which air drag acts on the drone body frame. For modeling drag along the drone's body axis, under assumed wind speeds $v_{w,z}$ in the range 2 - 8 m/s, a linear drag model is used:

$$F_{drag,i} = bv_i \tag{28}$$

where b is the linear drag coefficient and v_i is drone speed along each of x, y, z axis.

The nonlinear mechanical model, as seen in Fig. 1, is represented in the body frame of the drone as

$$m\ddot{x} = F_{\rm x} - F_{\rm drag_{xx}} \tag{29}$$

$$m\ddot{y} = F_{y} - F_{\text{drag}_{xy}} \tag{30}$$

$$m\ddot{z} = F_{\rm z} - mg - F_{\rm drag_z} \tag{31}$$

$$I_x \ddot{\phi} = \tau_\phi - (\dot{\theta} \dot{\psi} (I_y - I_z)) \tag{32}$$

$$I_{y}\ddot{\theta} = \tau_{\theta} - (\dot{\phi}\dot{\psi}(I_{z} - I_{x})) \tag{33}$$

$$I_z \ddot{\psi} = \tau_{\psi} - (\dot{\phi}\dot{\theta}(I_x - I_y)) \tag{34}$$

B. Fuel Reservoir-Engine Dynamics

By adopting a modeling approach that utilizes power conservation across the power interfaces of these components, the complexities associated with modeling the internal combustion engine and fuel reservoir are circumvented, eliminating the need to address unmodeled internal dynamics through an additional nonlinear term. By applying a power balance across each component we bridge unknown internal dynamics of hybrid powertrain subsystems:

$$\sum P_{out} = \eta \sum P_{in} \tag{35}$$

Eq. (35) tells us that the power flowing into the component (right-hand side) from the components (left-hand side) is conserved. For the hybrid powertrain, the chemical power of fuel must be equal to the power of the engine output

$$P_e = wT_e = \eta(\cdot)P_c = -\eta(\cdot)\dot{f}H_{LV} \tag{36}$$

where f is the flow of the fuel from the reservoir to the engine, H_{LV} is the lower heating value of the fuel (J/kg), and η is the coefficient of energy domain conversion efficiency. Engine output with added battery power is equal to the power needed by electrical motors

$$P_{el} = vi = \kappa(\cdot)(P_e + P_b) \tag{37}$$

where P_e is the power directly supplied by the engine to the motors, and P_b is the power taken from the engine by the battery. The electrical motor power is equal to the linear combination along each axis of mechanical power of the drone

$$P_{mech} = -\sum_{i} \psi_{i} F_{i} v_{i} = \zeta(\cdot) P_{el}$$
 (38)

where ψ_i is the linear power coefficient, F_i is the amplitude of force exerted by the rotors of the drone, v_i is the amplitude of the drone speed in the body reference frame along each axis $i \in \{x, y, z\}$. Finally, the model of the reservoir fuel flow is

$$\dot{f} = -\alpha(\cdot)F_x v_x - \beta(\cdot)F_y v_y - \gamma(\cdot)P_b - \frac{1}{T_f}f \tag{39}$$

where $\alpha(\cdot)$, $\beta(\cdot)$, and $\gamma(\cdot)$ combine and have a meaning of the power transmission coefficients (accumulated system inefficiencies) along the power flow of the powertrain. Continuing, we drop the brackets and treat α , β , γ as constants. Equation (39) has a bilinear nature as its terms are made of products of forces (control) and velocities(states). We moved the altitude z-axis out of Eq. (39) as stabilization of the zaxis along with rotational dynamics is controlled through the battery source. For slower dynamics like lateral dynamics, the battery source is seen as a disturbance that takes the power from the engine.

C. Lateral-Fuel Dynamics

Based on the previous sections' derivations, we finally form the state-space representation of the model that captures the dynamics of the drone along the z-axis of its body frame and has a connection with fuel reservoir dynamics

$$\dot{x} = v_x, x(0) = x_0
(40)$$

$$\dot{y} = v_y, y(0) = y_0
(41)$$

$$\dot{v}_x = \frac{1}{m} F_x - \frac{b_x}{m} v_x, v_x(0) = v_{x,0}
(42)$$

$$\dot{v}_y = \frac{1}{m} F_y - \frac{b_y}{m} v_y, v_y(0) = v_{y,0}
(43)$$

$$\dot{f} = -\alpha F_x v_x - \beta F_y v_y - \gamma P_b - \frac{1}{T_f} f, \qquad f(0) = f_0$$
(44)

For bilinear model Eqs. (40)-(44), we assume that the rotational dynamics of the drone are stable and have settled [3]. The drone's autopilot commanded thrust shows through F_x and F_y , Eqs. (24)-(25), and in our model these forces act as control inputs u_x and u_y . Product of u_x and state v_x , and analogously u_y and v_y is power delivered to lateral movement of the drone. Simultaneously, as a portion of the engine power is delivered to the battery, the battery power oscillations will be viewed as a disturbance $d_f = P_b$.

D. Fast Battery Linearizes Bilinear System

The integration of a fast energy source such as a battery and a slow energy source like a fuel generator provides a foundation for timescale separation. The battery, characterized by its rapid response and high power density, is capable of supplying instantaneous power demands, thus accommodating the fast dynamics of the drone's power requirements during maneuvers and transient operations. Conversely, the fuel generator, as it has a higher energy density and slower dynamic response, serves as a steady and reliable energy source for sustaining prolonged flight operations. Hybrid dual-energy source architecture enables the separation of timescales in the power management system. This enables the separation of timescales in Eqs. (40)-(44), where the fast dynamics influenced by the battery are seen as constant relative to the slower dynamics governed by the fuel generator, and vice-versa. Under the influence of a bounded battery disturbance, we derive composite control for the system (40)-(44) that can be first rewritten as

$$\dot{x} = v_x,
\dot{y} = v_y,
\dot{v}_x = \frac{1}{m} u_x - \frac{b_x}{m} v_x,
\dot{v}_y = \frac{1}{m} u_y - \frac{b_y}{m} v_y,
\dot{f} = -\alpha u_x v_x - \beta u_y v_y - \gamma d_f - \frac{1}{T_f} f$$

$$x(0) = x_0 \quad (45)$$

$$v_x(0) = y_0 \quad (47)$$

$$v_y(0) = v_{y,0} \quad (48)$$

$$f(0) = f_0 \quad (49)$$

where d_f is a battery-bound disturbance. Based on the the time-scale separation, we observe that the slow subsystem becomes a linear model as $\epsilon \rightarrow 0$, and from the fast subsystem (45)-(48) we obtain

$$\overline{v}_x = \frac{u_x}{b_x} \tag{50}$$

$$\overline{v}_x = \frac{u_x}{b_x} \tag{50}$$

$$\overline{v}_y = \frac{u_y}{b_y} \tag{51}$$

as the timescale becomes stretched $O(t/\epsilon) \to O(\tau)$ due the property of the timescale separation.

We now obtain the reduced "slow" order linear model

$$\dot{f}_s = -\alpha u_{x,s} \overline{v}_x - \beta u_{y,s} \overline{v}_y - \gamma \overline{d}_f - \frac{1}{T_f} f_s \qquad (52)$$

For this subsystem, we implement the slow policy $u_s =$ $[u_{x,s}, u_{y,s}]^T$ which can be blind or aware of battery disturbance. The "fast" system has the same form as Eqs. (42)-(43), and computed policy $u_f = [u_{x,f}, u_{y,f}]^T$ will always be blind towards battery disturbance. In the context of battery disturbance, fast control is LQR regulation. Together, slow and fast control at each timestep form an online composite policy $u_c = u_f + u_s$

IV. NUMERICAL RESULT

For the parameters of the system given in Tables (I-II), we compare the leftover fuel at the end of the flight of two online LQR policies against the unknown policy that was implemented during data collection experiments. The first of the two policies is the LQR without disturbance information, which we call "blind" and the second is "aware" LQR, as it has information about battery power disturbance on the fuel flow. We use time-scale separated models from the previous section with a discretization time-step of $\Delta T = 0.1$ s. The LQR controller quadratic cost terms are set to $Q_f =$ $Q_{T_f} = \operatorname{diag}([1,1,1,1])$, and $R_f = \operatorname{diag}([1,1])$ for the fast subsystem, and $Q_s=Q_{T_s}=0.1$, and $R_s=\mathrm{diag}([0.1,0.1])$ for the slow subsystem. Once controls for subsystems are computed separately, Eqs. (8)-(11), we add them and apply them to the model of the whole system Eqs. (45)-(49). Constraints on the maximal rate of change of states come from data, ensuring the control actions respect the system's physical limitations.

In Fig. 2, the lateral drone trajectory in the xy-plane during the cruise period of the flight mission is shown. The trajectory shows red dashed arrows in the direction of the

drone's lateral movement. The green dot is the start, and the blue dot end point of the cruise phase. The trajectory contains loops and changes in direction and the path does not appear to be smooth, indicating that the drone experienced disturbances and that the lateral control policy was not optimized. Following on our hypothesis, Fig. 3 shows how LQR control policies have more leftover fuel at the end of the flight compared to the unknown policy. In Fig. 4 we observe how composite control saved approximately 3.5-4.5%of the fuel level compared to the beginning of the cruise flight phase, with the blind policy on the lower-end and disturbance-aware policy as the best fuel-saving policy.

TABLE I FAST SUBSYSTEM PARAMETERS AND THEIR UNITS

		Fast Subsystem Parameters			
			b_y [N·s/m]		
ĺ	20.8953	1.7046	1.6218		

TABLE II SLOW SUBSYSTEM PARAMETERS AND THEIR UNITS

Slow Subsystem Parameters					
α [l/sW]	β [l/sW]	γ [l/sW]	T_f [1/s]		
0.005594	0.003626	0.0025	396.2434		

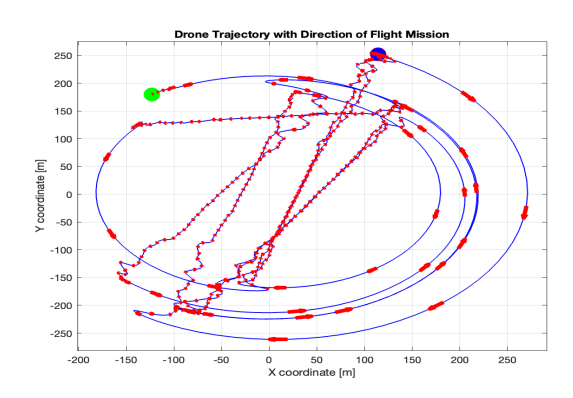


Fig. 2. Lateral trajectory of the drone with unknown control from flight mission measurements

V. CONCLUSION

Our paper proposes a novel model that captures the interaction of lateral dynamics and powertrain energy conversion dynamics. We emphasize how different rates of operation of energy sources play a distinct role in the linearization of the derived nonlinear model. This leads to the application of near-optimal composite control with disturbance awareness through which we show reduced fuel consumption. The downside of the disturbance-aware LQR is dependence on the accurate system model and reliable disturbance prediction which we plan to further explore and relax in the future.

VI. ACKNOWLEDGMENTS

The authors gratefully acknowledge the contribution of Lincoln Lab and LL MIT team comments.

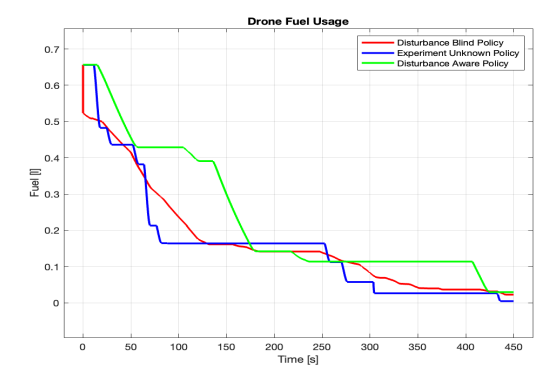


Fig. 3. Leftover fuel during the flight

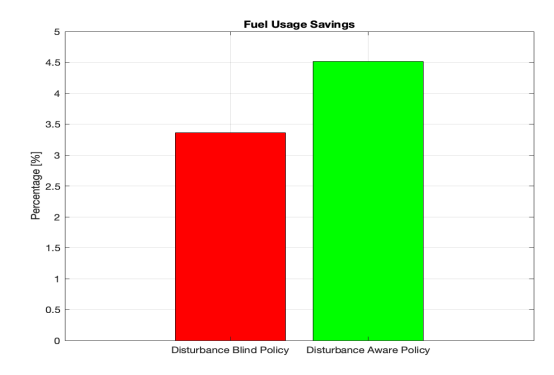


Fig. 4. Fuel saving comparison a) battery blind policy b) battery aware policy

REFERENCES

- [1] Sylvain Bertrand et al. "A hierarchical controller for miniature VTOL UAVs: Design and stability analysis using singular perturbation theory". In: *Control Engineering Practice* 19.10 (2011), pp. 1099–1108.
- [2] Luis Rodolfo García Carrillo et al. *Quad rotor-craft control: vision-based hovering and navigation*. Springer Science & Business Media, 2012.
- [3] Robert E. Mahony, Vijay R. Kumar, and Peter Corke. "Multirotor Aerial Vehicles: Modeling, Estimation, and Control of Quadrotor". In: *IEEE Robotics & Automation Magazine* 19 (2012), pp. 20–32. URL: https://api.semanticscholar.org/CorpusID:1081012.
- [4] Eduardo Gamaliel Hernández-Martínez et al. "Trajectory tracking of a quadcopter UAV with optimal translational control". In: *IFAC-PapersOnLine* 48.19 (2015), pp. 226–231.
- [5] Pedro Castillo, Rogelio Lozano, and Alejandro Enrique Dzul. *Modelling and control of mini-flying machines*. Springer Science & Business Media, 2005.
- [6] Juan Escareno, Sergio Salazar-Cruz, and Rogelio Lozano. "Embedded control of a four-rotor UAV". In: 2006 American Control Conference. IEEE. 2006, 6-pp.

- [7] Anton A Pyrkin et al. "Output controller for quadcopters based on mathematical model decomposition".
 In: 22nd Mediterranean Conference on Control and Automation. IEEE. 2014, pp. 1281–1286.
- [8] Minh Quan Huynh, Weihua Zhao, and Lihua Xie. "L 1 adaptive control for quadcopter: Design and implementation". In: 2014 13th International Conference on Control Automation Robotics & Vision (ICARCV). IEEE. 2014, pp. 1496–1501.
- [9] Dmitri Aleksandrov and Igor Penkov. "Energy consumption of mini UAV helicopters with different number of rotors". In: 11th International Symposium" Topical Problems in the Field of Electrical and Power Engineering. 2012, pp. 259–262.
- [10] Yukai Chen et al. "A case for a battery-aware model of drone energy consumption". In: 2018 IEEE international telecommunications energy conference (INT-ELEC). IEEE. 2018, pp. 1–8.
- [11] Fouad Yacef et al. "Optimization of energy consumption for quadrotor UAV". In: *Proceedings of the International Micro Air Vehicle Conference and Flight Competition (IMAV), Toulouse, France.* 2017, pp. 18–21.
- [12] Rashid Alyassi et al. "Autonomous recharging and flight mission planning for battery-operated autonomous drones". In: *IEEE Transactions on Automation Science and Engineering* 20.2 (2022), pp. 1034–1046.
- [13] E Abed. "Decomposition and stability for multiparameter singular perturbation problems". In: *IEEE transactions on Automatic Control* 31.10 (1986), pp. 925–934.
- [14] J. Chow and P. Kokotovic. "A decomposition of near-optimum regulators for systems with slow and fast modes". In: *IEEE Transactions on Automatic Control* 21.5 (1976), pp. 701–705. DOI: 10.1109/TAC.1976.1101342.
- [15] Samuel Pfrommer and Somayeh Sojoudi. "LQR Control with Sparse Adversarial Disturbances". In: 2022 IEEE 61st Conference on Decision and Control (CDC). IEEE. 2022, pp. 2346–2353.
- [16] Dimitri Bertsekas. *Dynamic programming and optimal control: Volume I.* Vol. 4. Athena scientific, 2012.
- [17] Gautam Goel and Babak Hassibi. "The power of linear controllers in LQR control". In: 2022 IEEE 61st Conference on Decision and Control (CDC). IEEE. 2022, pp. 6652–6657.
- [18] Gautam Goel and Babak Hassibi. "Competitive control". In: *IEEE Transactions on Automatic Control* (2022).
- [19] Marija D Ilić and Rupamathi Jaddivada. "Multilayered interactive energy space modeling for nearoptimal electrification of terrestrial, shipboard and aircraft systems". In: *Annual Reviews in Control* 45 (2018), pp. 52–75.